Peltier effect in doped silicon microchannel plates*

Ci Pengliang(慈朋亮)[1], Shi Jing(石晶)[1], Wang Fei(王斐)[1], Xu Shaohui(徐少辉)[1], Yang Zhenya(杨振亚)[1], Yang Pingxiong(杨平雄)[1], Wang Lianwei(王连卫)[1,†], Gao Chen(高晨)[2], and Paul K. Chu(朱剑豪)[3]

[1]Laboratory of Polar Materials and Devices, Ministry of Education, and Department of Electronic Engineering, East China Normal University, Shanghai 200241, China
[2]Department of Microelectronics, Fudan University, Shanghai 200433, China
[3]Department of Physics and Material Sciences, City University of Hong Kong, Tat Chee Avenue, Kowloon, Hong Kong, China

Abstract: The Seebeck coefficient is determined from silicon microchannel plates (Si MCPs) prepared by photo-assisted electrochemical etching at room temperature (25 ℃). The coefficient of the sample with a pore size of 5 × 5 μm^2, spacing of 1 μm and thickness of about 150 μm is –852 μV/K along the edge of the square pore. After doping with boron and phosphorus, the Seebeck coefficient diminishes to 256 μV/K and –117 μV/K along the edge of the square pore, whereas the electrical resistivity values are 7.5×10^{-3} Ω·cm and 1.9×10^{-3} Ω·cm, respectively. Our data imply that the Seebeck coefficient of the Si MCPs is related to the electrical resistivity and is consistent with that of bulk silicon. Based on the boron and phosphorus doped samples, a simple device is fabricated to connect the two type Si MCPs to evaluate the Peltier effect. When a proper current passes through the device, the Peltier effect is evidently observed. Based on the experimental data and the theoretical calculation, the estimated intrinsic figure of merit *ZT* of the unicouple device and thermal conductivity of the Si MCPs are 0.007 and 50 W/(m·K), respectively.

Key words: silicon microchannel plates; doping; thermoelectric; Peltier effect
DOI: 10.1088/1674-4926/32/12/122003 **PACC:** 6140G; 7220P; 7360J

1. Introduction

There has been increasing interest in thermoelectric materials due to international concerns about environmental deterioration and alternative energy. A thermoelectric device can generate power using heat from industrial waste and automobile exhausts[1]. These devices can also be utilized in noise and vibration-free refrigerators with zero greenhouse gas emissions. Owing to its large potential, there has been extensive research to investigate and identify materials with desirable thermoelectric characteristics[2–5]. Unfortunately, the very high thermal conductivity (about 150 W/(m·K) at room temperature) limits the applications of silicon as a thermoelectric material[6]. However, silicon nanowires, which possess reduced thermal conductivity and enhanced thermoelectric efficiency on account of the quantum confinement effect inherent to nanomaterials, may be more suitable[7–9]. Nevertheless, since it is challenging to make the good electrical connection between the silicon nanowire arrays and contacts necessary for the thermoelectric modules[10], no power generation or refrigeration devices based on silicon nanowires have been reported until now. Bulk materials such as Bi_2Te_3 are still mainstream in practical applications such as semiconductor refrigeration. Unlike silicon nanowires, silicon microchannel plates (Si MCPs) with low thermal conductivity arising from the porous structure[11, 12] can be easily fabricated into different types of thermoelectric devices similar to bulk materials. In this work, we investigate the effects of boron and phosphorus doping on the thermoelectric properties of Si MCPs. The pore size of the Si MCPs is 5 × 5 μm^2 and their spacing is 1 μm. The Seebeck coefficient and electrical resistivity are measured at room temperature (25 ℃) and, in order to elucidate the Peltier effect, the p-type and n-type Si MCPs are connected by a copper sheet to form the thermoelectric junction.

2. Experimental details

The Si MCPs were prepared by photo-assisted electrochemical etching (PAECE). The starting substrate was a single-side polished p-type ⟨100⟩ silicon wafer with an electrical resistivity of 2–9 Ω·cm and thickness of 500 μm. The wafer was thermally oxidized to form an oxide layer of 300 nm and then patterned using photolithography. A buffered hydrofluoric acid (BHF) solution was used to etch windows in the oxide layer. The wafer was then immersed into a 25 wt% tetramethyl ammonium hydroxide (TMAH) solution at 85 ℃ for a few minutes to form the inverted pyramidal structures on the silicon. After the oxide layer had been completely removed by

* Project supported by the Shanghai Fundamental Key Project (No. 10JC1404600), the Shanghai Natural Science Foundation (No. 11ZR1411000), the Innovation Program of Shanghai Municipal Education Commission (No. 09ZZ46), the International Collaboration Project (No. 10520704400), the National Natural Science Foundation of China (Nos. 60990312, 61076060, 61176108), and the City University of Hong Kong Strategic Research Grant (SRG) (No. 7008009).
† Corresponding author. Email: lwwang@ee.ecnu.edu.cn
Received 21 April 2011, revised manuscript received 16 June 2011

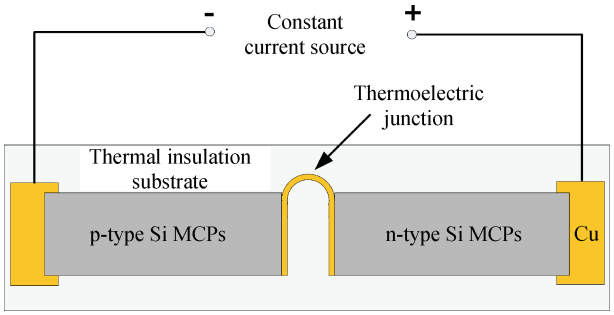

Fig. 1. Schematic diagram of the device with the thermoelectric junction formed by p-type and n-type Si MCPs.

the BHF solution, PAECE was performed for 8 h at 20 ℃ in order to break off the microchannel layer from the silicon substrate. More details about the experimental procedures can be found in Ref. [13]. The samples were designated as A. The microstructure of the samples was characterized by scanning electron microscopy (SEM).

Some of the Si MCPs were then doped with boron at 1180 ℃ for 3 h and that sample was designated as sample B. Nitrogen gas was used as the protective gas to prevent oxidation and borosilicate glass was the diffusion source. Another MCP sample doped with phosphorus using $POCl_3$ as the liquid source at 1100 ℃ for 30 min was designated as C. The electrical resistivity of the doped samples was determined by using a four-point probe at room temperature.

The samples were then cut into 1 cm long and 0.4 cm wide pieces using a laser beam for subsequent studies. Before characterization, they were placed on a thermally insulated substrate while two copper sheets serving as both the thermally and electrically conducting layers were spring-loaded onto the sample by probes. The time evolution of the thermo-electromotive force was monitored by a digital multimeter and the temperature was determined by a K-type thermocouple thermometer.

A typical device was fabricated to investigate the Peltier effect. One side of the device was the p-type Si MCPs and the other side was the n-type Si MCPs. They were connected by a U-shaped copper sheet and conductive silver paste (DAD-40) was used to glue the parts together, as shown in Fig. 1. The temperature of the junction was determined by measuring the temperature of the U-shaped copper sheet with a thermocouple thermometer.

3. Results and discussion

Figure 2 depicts the surface and cross-sectional views of the Si MCPs on the micro as well as macro scales. Pores of about 5×5 μm^2 in size were distributed in a square lattice and the spacing between two pores was about 1 μm, as shown in Figs. 2(a) and 2(b). The thickness of the Si MCPs was about 150 μm, which can be clearly observed from Fig. 2(c). Figure 2(d) shows the entire Si MCPs and substrate with a diameter of 10 cm. The electrical resistivity values of samples A (undoped), B (boron doped) and C (phosphorus doped) are 1.5×10^5 Ω·cm, 7.5×10^{-3} Ω·cm and 1.9×10^{-3} Ω·cm, respectively.

The Seebeck coefficient of samples can be determined

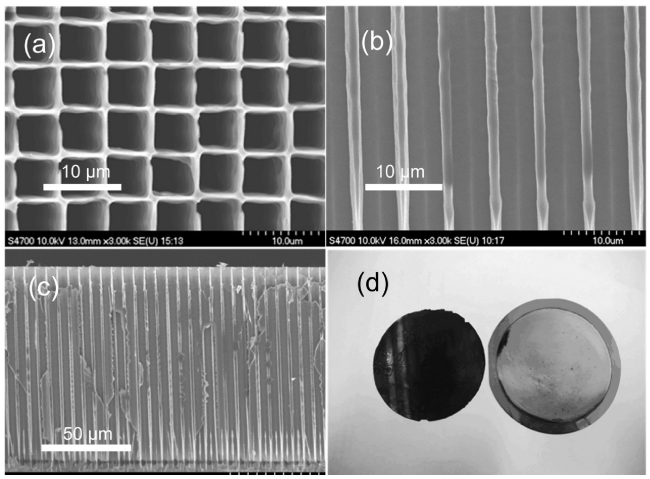

Fig. 2. SEM images of (a) surface, (b) and (c) cross-section as well as (d) the microscope image of Si MCPs and substrate with a diameter of 10 cm.

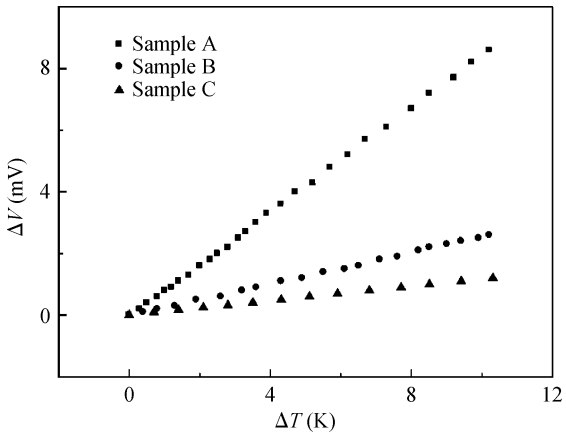

Fig. 3. ΔT–ΔV plots of the doped and undoped samples.

from the thermoelectromotive force (ΔV) and temperature difference (ΔT) by $S = \Delta V/\Delta T$. In other words, the slope of the ΔT–ΔV plot represents the Seebeck coefficient[14]. The ΔT–ΔV plots of the doped and undoped samples are depicted in Fig. 3. The Seebeck coefficients of samples A, B, and C are –852, 256, and –117 μV/K, respectively. Compared to the corresponding resistivity of 1.5×10^5 Ω·cm, 7.5×10^{-3} Ω·cm and 1.9×10^{-3} Ω·cm, it is clear that the absolute value of the Seebeck coefficient decreases when the electrical resistivity of the Si MCPs decreases. In addition, both the resistivity, which has the same order of magnitude of that of intrinsic silicon (about 2.5×10^5 Ω·cm at room temperature), and the negative Seebeck coefficient of sample A indicate that Si MCPs prepared by PAECE are no longer p-type but instead resemble intrinsic silicon. It may be due to the depletion of carriers resulting from the surface states of the Si MCPs. Moreover, according to the Seebeck coefficient and electrical resistivity, the power factor (S^2/ρ) of samples B and C are 8.7×10^{-1} and 7.2×10^{-1} mW/(m·K), respectively. Thus, the concentration and type of the dopant are important to the power factor.

Using the simple device with a thermoelectric junction formed by the boron and phosphorus doped Si MCPs, a current

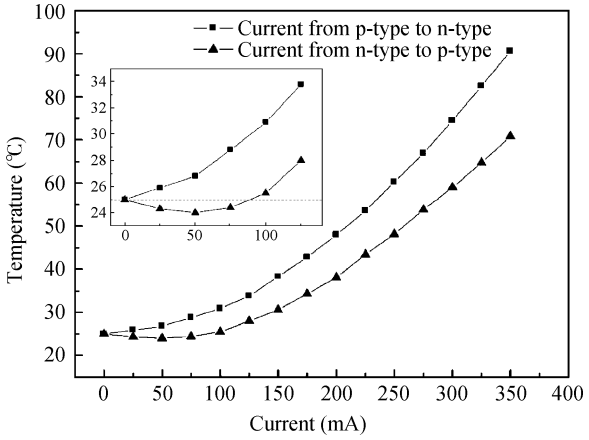

Fig. 4. Relationship between the temperature at the thermoelectric junction and the positive/negative current with the inset showing the magnified graph from 0 to 125 mA.

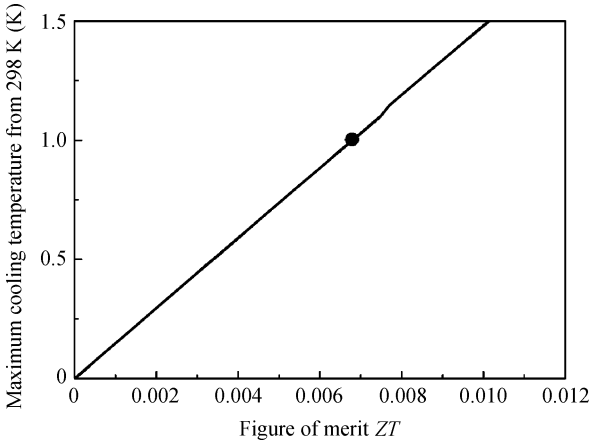

Fig. 5. Thermoelectric maximum temperature differentials versus 298 K figure-of-merit ZT for a standard two-leg thermoelectric cooler. The black circle corresponds to the present experimental results from Si MCPs thermoelectric junction.

is introduced to evaluate the Peltier effect. When an electrical current flows from the n-type to the p-type sides, both electrons in the n-type Si MCPs and holes in the p-type Si MCPs flow away from the junction. Both carriers conduct heat away from the junction, which then cools. However, the junction is heated if the direction of the current is reversed. The relationship between the temperature and current is illustrated graphically in Fig. 4. When the current flowing from the n-type to p-type sides is below 100 mA, a temperature below 25 ℃ can be observed. The maximum temperature difference in this range is about 1 ℃ while the current is around 50 mA, as shown in the inset in Fig. 4. However, the Peltier effect in this range is still very weak. When the current from the n-type side to the p-type side is over 100 mA, the temperature at the junction rises to above 25 ℃ indicating that Joule heating is more dominant than that arising from the Peltier effect. In order to further study the Peltier effect, the direction of the current is reversed. Under these conditions, Peltier heating and Joule heating are coupled at the junction. Compared to the situation in which the current flows from the n-type side to the p-type side, a much higher temperature is observed at the same current. The temperature difference between the two directions becomes more evident as the current increases. As shown in Fig. 4, the temperature difference is 19.8 ℃ when the current is 350 mA. This temperature difference can be attributed to double Peltier heating.

The intrinsic figure of merit ZT of a unicouple and thermal conductivity of the p-type and n-type MCP legs are estimated by comparing the theoretically calculated and experimental results. As shown in Refs. [2, 15], the cooling power Q_c at the heat source of the unicouple can be obtained by the following relationship:

$$Q_c = (S_P - S_n) I T_C - K(T_H - T_C) - I^2 R/2, \qquad (1)$$

where S_p and S_n are the Seebeck coefficients of the p-type and n-type parts, respectively, T_H and T_C are the temperature at the hot and cold junctions, respectively, I is the electrical current flowing through each thermoelectric leg of the device, K and R are the total thermal conductance and electrical resistance of the unicouple, respectively, and can be expressed as the simple relationship $K = K_P + K_N$, and $R = R_P + R_N$, if the parasitic factors such as contact resistances and contact thermal conductance, etc. are negligible, and K_P (K_N) and R_P (R_N) are the thermal conductance and electrical resistance of the individual p-type and n-type legs, respectively. A maximum temperature difference $\Delta T_{max} = T_H - T_C$ is obtained by setting $(Q_c)_{max} = 0$,

$$\Delta T_{max} = Z T_C^2/2, \qquad (2)$$

and the minimum attainable temperature $(T_C)_{min}$ can be solved using Eq. (2):

$$(T_C)_{min} = (\sqrt{1 + 2ZT_H} - 1)/Z, \qquad (3)$$

when the figure of merit ZT of a pair of thermoelectric materials is given as

$$ZT = \frac{(S_P - S_N)^2 T}{(\sqrt{\kappa_P \rho_P} + \sqrt{\kappa_N \rho_N})^2}, \qquad (4)$$

where k_P (k_N) and ρ_P (ρ_N) are the thermal conductivity and electrical resistivity of the individual p-type and n-type legs, respectively.

The calculated maximum cooling values from 298 K for a standard intrinsic two-leg thermoelectric refrigerator versus the 298 K intrinsic ZT values are shown in Fig. 5. Corresponding to the experimental maximum temperature difference ($\Delta T = 1$) of the two-legged thermoelectric junction device based on the Si MCPs, the intrinsic ZT value is equal to 0.007, as indicated by the black circle in Fig. 5. Since the p-type and n-type Si MCPs are fabricated from the same Si MCP samples (almost intrinsic) by doping, they have the same thermal conductivity due to identical structures. The thermal conductivity of the Si MCPs can be obtained to be $\kappa = 50$ W/(m·K) from Eq. (4). The Si MCP structures have a thermal conductivity value lower than that of bulk Si (about 150 W/(m·K)) at room temperature and the value is similar to that of the periodic microporous silicon films prepared by a silicon-on-insulator (SOI) process[12]. The results indicate that MCP structure can indeed reduce the thermal conductivity in silicon. However, the figure of merit ZT is not increased substantially. The value may be increased by reducing the pore size or spacing between the pores by oxidation of the Si MCPs to produce nano-scale structures.

4. Conclusion

Si MCPs are prepared by photo-assisted electrochemical etching (PAECE) and doped with boron and phosphorus. The Seebeck coefficient is directly related to the electrical resistivity of the Si MCPs similar to bulk silicon. A test device consisting of the p-type and n-type Si MCPs is fabricated and the Peltier effect is observed as current flows. By changing the current direction, the larger current gives rise to a bigger temperature difference due to double Peltier heating. The high electrical resistivity (compared to other matural thermoelectric materials) of the Si MCPs seems to be a key impediment to the application of thermoelectric devices. However, the Seebeck coefficient and electrical resistivity can be further optimized by adjusting the impurity concentration and another dopant such as antimony may be more suitable in order to achieve a low electrical resistivity and acceptable Seebeck coefficient. In addition, the thermal conductivity of the Si MCPs derived from the theoretical calculation confirms that the MCP structure is effective in reducing the thermal conductivity.

Acknowledgements

The authors would like to extend their sincere thanks to Prof. Qu Xinping (Fudan University) for conducting the phosphorus doping work.

References

[1] DiSalvo F J. Thermoelectric cooling and power generation. Science, 1999, 285: 703

[2] Harman T C, Taylor P J, Walsh M P, et al. Quantum dot superlattice thermoelectric materials and devices. Science, 2002, 297: 2229

[3] Hsu K F, Loo S, Guo F, et al. Cubic $AgPb_mSbTe_{2+m}$: bulk thermoelectric materials with high figure of merit. Science, 2004, 303: 818

[4] Watanabe T, Hasaka M, Morimura T, et al. Thermoelectric properties of the Co-doped β-$FeSi_2$ mixed with Ag. J Alloys Compd, 2006, 417: 241

[5] Joshi G, Lee H, Lan Y C, et al. Enhanced thermoelectric figure-of-merit in nanostructured p-type silicon germanium bulk alloys. Nano Lett, 2008, 8(12): 4670

[6] Weber L, Gmelin E. Transport properties of silicon. Appl Phys A, 1991, 53: 136

[7] Hochbaum A I, Chen R K, Delgado R D, et al. Enhanced thermoelectric performance of rough silicon nanowires. Nature, 2008, 451: 163

[8] Zhang G, Zhang Q X, Bui C T, et al. Thermoelectric performance of silicon nanowires. Appl Phys Lett, 2009, 94: 213108

[9] Shi L H, Yao D L, Zhang G, et al. Size dependent thermoelectric properties of silicon nanowires. Appl Phys Lett, 2009, 95: 063102

[10] Lee J H, Galli G A, Grossman J C. Nanoporous Si as an efficient thermoelectric material. Nano Lett, 2008, 8(11): 3750

[11] Gesele G, Linsmeier J, Drach V, et al. Temperature-dependent thermal conductivity of porous silicon. J Phys D: Appl Phys, 1997, 30: 2911

[12] Song D, Chen G. Thermal conductivity of periodic microporous silicon films. Appl Phys Lett, 2004, 84(5): 687

[13] Yuan D, Ci P L, Tian F, et al. Large-size P-type silicon microchannel plates prepared by photoelectrochemical etching. J Micro/Nanolith MEMS MOEMS, 2009, 8(3): 033012

[14] Salleh F, Asai K, Ishida A, et al. Seebeck coefficient of ultrathin silicon-on-insulator layers. Appl Phys Express, 2009, 2: 071203

[15] Rowe D M. CRC handbook of thermoelectrics. Boca Raton: CRC Press Inc, 1995